

# 11T DIPOLE SHORT MODEL COIL METROLOGY AT COLD AND MEASUREMENT OF ITS THERMAL CONTRACTION

D. Mergelkuhl<sup>#</sup>, J-Ch. Gayde, K. Nikolitsas, CERN, Geneva, Switzerland

## Abstract

The main objective of the HL-LHC project at CERN is to increase the LHC peak luminosity by a factor of five and the integrated luminosity by a factor of ten. The increased integrated and peak luminosity requires to improve the cleaning efficiency of the collimation system with the installation of new collimators in the cold section of the machine. In order to create the space for such equipment a set of two new high field magnet (here referred as 11T dipole) will replace one standard LHC dipole leaving free space in middle for the new equipment.

The metrology tests of one of the 11T dipole short model coils (1.97 m long) have been performed at CERN, using close range photogrammetric techniques, in order to evaluate the mechanical behaviour of the coil. For this measurement, the coil has been immersed and completely covered by nitrogen gas for the thermal cycling ( $\Delta T \approx 178$  K).

In this paper, some of the environmental constraints are highlighted. These constraints have been: a thin vapour cloud on the top of the cryostat, a small ice layer that has been formed a few minutes after the opening of the cryostat cap and the high temperature gradient for measurement rays. As result, it can be concluded that the short model coil of the 11T dipole is a flexible structure that contracts and bends (bending of 4.85 mm between warm and cold state of the coil). In addition, the best estimate for the coefficient of thermal expansion of the coil is  $12.8 \mu\text{m}/\text{m}/\text{K}$  what is probably not enough to characterize the short model coil as a composite structure.

## INTRODUCTION

The High-Luminosity Large Hadron Collider (HL-LHC) project aims to boost the performance of the LHC in order to enhance the potential for discoveries after 2027. The objective is to increase luminosity by a factor of 10 beyond the LHC's design value [1].

Luminosity is an important indicator of the performance of an accelerator: it is proportional to the number of collisions that occur in a given amount of time. The higher the luminosity, the more data the experiments can gather to allow them to observe rare processes. The High-Luminosity upgrade of the Large Hadron Collider (HL-LHC) requires new dipole magnets (see Fig. 1) with a conductor peak field of 11T. One of the main parts of these dipoles are the coils. The dipole magnets are in contact via the loading plates, indicated in blue in Fig. 1, with the pole wedge. The coil design and construction are explained in detail in [2]. A part of the development procedure is the study of the performance limitation observed after

powering runs of the 11T series magnets (namely S2, S3 and S4) including thermal cycles [3].

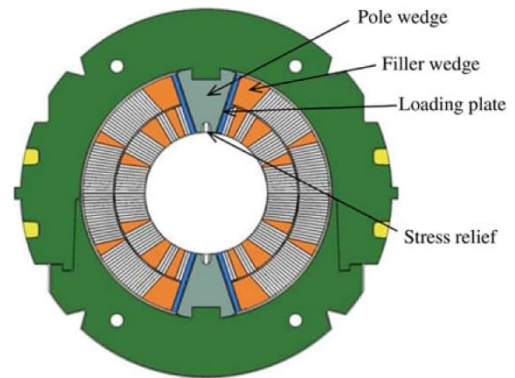


Figure 1: Collared coil concept of the 11T dipole magnet

Because a full coil is a composite assembly [4], a short model coil (coil C122)  $\sim 1.97$  m long has been measured at cold conditions to determine the coefficients of thermal expansion (CTE) of this object. In order to study the mechanical behaviour of the 11T dipole short model coil during the thermal cycle, the close range photogrammetric techniques have been used in a series of four measurement:

- M<sub>1</sub>: February 1<sup>st</sup>, 14<sup>h</sup>12-14<sup>h</sup>32, Warm Measurement
- M<sub>2</sub>: February 2<sup>nd</sup>, 13<sup>h</sup>50-14<sup>h</sup>01, Cold Measurement
- M<sub>3</sub>: February 3<sup>rd</sup>, 14<sup>h</sup>15-14<sup>h</sup>36, Warm Measurement
- M<sub>4</sub>: February 11<sup>th</sup>, 14<sup>h</sup>28-14<sup>h</sup>45, Warm Measurement

The specific time series of measurements has been chosen so that the thermal cycle (cool down and warm up) was carried out with a stable temperature difference in a fixed time interval. The M<sub>4</sub> measurement series has been added in order to ensure that the internal temperature of the coil has been fully recovered after the warm up and to verify the repeatability of the results from the M<sub>3</sub> measurement series. Thus, the purpose of this paper is to explain the measurement approach, to determine the deformations of the coil and to estimate the CTE after the cool down.

## APPLICATION

### Preparation of measurement setup

The team of the cryogenic laboratory at CERN has prepared the cryogenic test setup. The 11T dipole short model coil has been placed on isostatic supports (1 support point on the connection side and 2 support points on the opposite side) in an open cryostat (see Fig. 2). Due to this supporting system, the 11T short model coil was able to dilate and contract freely without any constraints. The cryostat has been covered during the cool down and the

<sup>#</sup>Dirk.Mergelkuhl@cern.ch



warm up with Plexiglas plates. The cool down has been done using a liquid nitrogen and the coil stayed in the cold nitrogen gas. The cryostat has been opened temporarily for the measurements.

The CERN Geodetic Metrology group proposed a measurement solution based on close range photogrammetry. The advantages of a non-contact measurement method with a relatively short acquisition time have been the main arguments. As the points have to be reproducible in 3D for the deformation analysis and the calculation of the CTE, it is necessary to have the corresponding signalisation that resists to the cool down and warm up procedure. To validate the measurement process a warm/cold cycle with a dummy load, represented by a stainless steel tube has been measured prior to the 11T coils. In this setup different sticker targets and target diameters could be tested. In parallel, the effective data acquisition time slot has been evaluated that is limited by the forming ice layer on the targets. Further the degradation of the measurement precision of the cold measurement caused by the high temperature gradient of the measurement rays could be assessed based on the results of the bundle adjustment. The vapour cloud on the top of the cryostat stabilizes after a short time and reduces slightly the contrast of the targets without compromising the measurement.



Figure 2: The setup for 11T short model coil cold test at CERN

### Photogrammetric setup

For all measurement series, the photos have been taken in parallel with two cameras by two operators to speed up the data acquisition: a) Canon 5DS and b) Nikon D3X. Both of them have been equipped with 28 mm lens. This procedure increases the redundancy and reliability of the measurement process. In addition, four carbon fibre scale bars with 10 reference scales have been placed outside the cryostat at room temperature. The scales have been installed slightly higher than the cryostat edge to avoid that the overflowing cold nitrogen gas reaches them, which would change the calibrated distances and add a layer of humidity or ice on the targets of the scale bars. In addition, this ice layer proscribes the use of retro-reflective targets

and forces the use of black and white stickers that have the inconvenience to generate more parasitic measurements due to reflection etc. The calculations have been performed with the digital photogrammetric workstation (DPA Professional module) of Hexagon.

Nearly 472 non-coded points have been placed in the critical areas on the 11T dipole coil. Additional 134 coded targets have been added to include the scale bars and to automatize the measurement process.

The following type of targets have been used for the coil:

- Self-adhesive paper stickers on rounded coil surface with a thickness of 100  $\mu\text{m}$  and a diameter of 2 mm to limit the non-flatness of the target to less than  $\pm 5$  microns.
- Self-adhesive foil stickers on the loading plates with a thickness of 70  $\mu\text{m}$  and a diameter of 3 mm that proved to stick better on the surfaces of the loading plates.

### Temperature data

Ten temperature sensors have been installed on the surface of the 11T short model coil by the team of the cryogenic laboratory at CERN. In the Table 1 below the average temperatures of all sensors and the maximum  $\Delta T$  between the sensors for each set of measurements are illustrated.

The measurement in the cold condition shows an inhomogeneous temperature distribution of the coil that has a significant influence on the calculation of the thermal contraction and the precision of the temperature measurement should be considered as important as the 3D measurement.

Table 1: The temperature data

Series	Max – Min (K)	Average (K)	$\Delta T$ (K)
M <sub>1</sub> -Warm	1.3	291.81 $\pm$ 0.17	M <sub>2</sub> - M <sub>1</sub> = - 177.68
M <sub>2</sub> -Cold	14.8	114.13 $\pm$ 3.81	M <sub>3</sub> - M <sub>2</sub> = - 177.54
M <sub>3</sub> -Warm	1.6	291.67 $\pm$ 0.29	M <sub>3</sub> - M <sub>1</sub> = - 0.14
M <sub>4</sub> -Warm	0.8	288.62 $\pm$ 0.16	M <sub>4</sub> - M <sub>1</sub> = - 3.19

### Coordinate system

A local right handed Cartesian coordinate system has been established using the first set of measurement (M<sub>1</sub>) in warm conditions on 1<sup>st</sup> of February.

For the measurements M<sub>2</sub>, M<sub>3</sub> and M<sub>4</sub> a best-fit transformation using a 6-DOF (3 translations, 3 rotations) has been done to get in the same coordinate system:

**Origin:** Intersection of the best-fit cylinder axis and the mean plane of the targets on the connection side end.

**Z - axis:** The calculated best-fit cylinder axis.

**Y - axis:** In direction of the loading plates. The average angle of the calculated mean planes of the two loading plates in XY-plane is defined as 0°. Positive to the top.

**X - axis:** Perpendicular to the two others in a right-handed Cartesian Coordinate System.

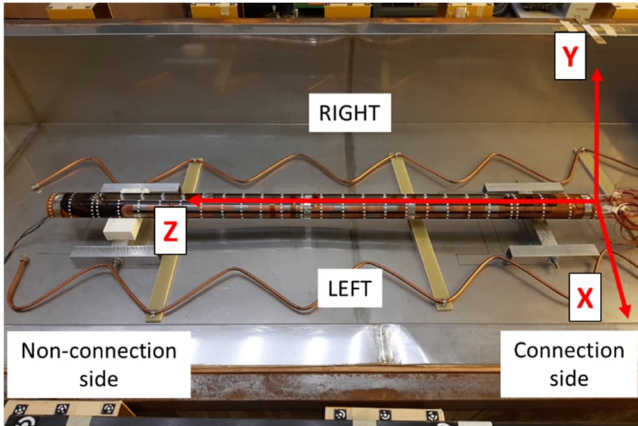


Figure 3: Definition of the Coordinate system

### Distribution of measured points

The non-coded targets on the differently oriented surfaces of the coil have been distributed as follows:

- 3x profiles on the non-connection end (13 points per cross section)
- 4x profiles on the connection end (13 points per cross section)
- 21x profiles (every 75 mm) in the area of the loading plates with 12 targets per cross section and 4 additional targets in the loading plate area
- 2 layers of 10 targets per end face
- 2x2 targets on the key surfaces

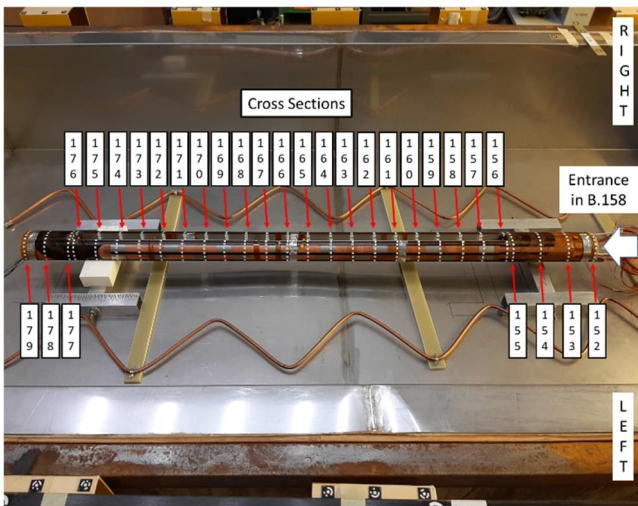


Figure 4: Numbering of the cross sections on the cylindrical surface of the coil

The numbering of the cross sections is illustrated in Fig. 4. In total 28 cross sections have been created on the cylinder surface (152 up to 179). This numbering starts from the connection end to the opposite end. The naming of the points starts from the left to right viewed from the connection side.

The measured points on the cross sections have been named with the following abbreviations {XXX}{YY}. Where {XXX} is the number of the cross section (152 up to 179) and {YY} is the number of the non-coded target.

Twelve points have been installed per cross section for the profiles 152 up to 155 and 177 up to 179. The number of points has been increased to 16 for cross sections 156 up to 176. Point numbers are counted from left to right with respect to the connection side.

For the cross sections in the loading plates area (156 up to 176) the targets with number 07, 08, 09 and 10 have been on the loading plate surfaces. 23 targets have been glued on the connection end surface of the coil and 23 targets have been glued on the non-connection end.

In total **472 targets** have been glued on the different surfaces of the 11T short model coil.

### Measurement configuration and statistical data

In average 600 points have been measured and more than 400 photos taken per project. For the warm measurements around 110 000 observations have been used and approximately 70000 for the cold measurement. In Fig. 5, the configuration of the camera positions and the point distribution is illustrated. The highly redundant measurement allows the automatic blunder detection on statistical values. The a posteriori standard deviation of the residuals for the image coordinates is slightly below 0.1 pixel with similar values for the measurements at room temperature and at cryogenic condition. In the final calculations, the maximal residuals for the scale bar distances have not been exceeding 15  $\mu\text{m}$  for any of the measurements. The a posteriori sigma of the measured scale bar distances is at the level of 8  $\mu\text{m}$ .

The mean standard deviations for the object coordinates are 5-10  $\mu\text{m}$  for the projects in warm conditions and the values increase by 50% for the cold project, which is caused by the reduced number of observations (~35% less), the reduced time slot and the vapour cloud. Due to the heterogeneous point distribution and reduced visibility for several points, the maximal corresponding values reach around 30  $\mu\text{m}$  for the projects at room temperature. For the project in cryogenic conditions, nearly 1% of the points had to be excluded due to an insufficient configuration. Even after their exclusion the maximal value of 51  $\mu\text{m}$  is still significantly higher than for the warm measurements.

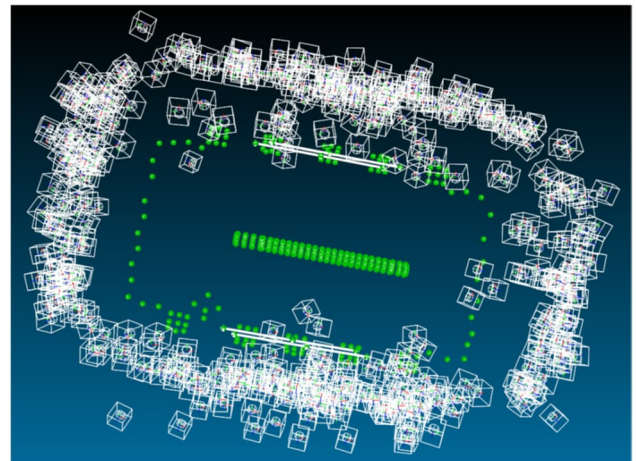


Figure 5: Configuration of camera positions (white) and point positions (green) for series M1

## ESTIMATION OF THE CTE

To calculate the thermal expansion coefficient of the 11T dipole short model coil the scale factor has been calculated from the 7-parameter transformation of the series M2 to M1. The abbreviation for the calculated scale factor is the following:

$$m_{AB} \pm \sigma_{m_{AB}} \quad (1)$$

Where:

- m: The scale factor
- $\sigma_m$ : The uncertainty of the scale factor
- A: Coil
- B: M<sub>2</sub> to M<sub>1</sub>, 7-parameter transformation between the measurement series

Thus, the coefficient of thermal expansion (mm/m/K) [5], is calculated by the following equation:

$$CTE_{AB} = \frac{m_{AB}}{\Delta T_B} \quad (2)$$

Where:

$\Delta T$ : The temperature difference between the measurement series (K).

The uncertainty of the coefficient of thermal expansion is given by equation 3.

$$\sigma_{CTE_{AB}} = \pm \sqrt{\left(\frac{1}{\Delta T_B}\right)^2 \cdot \sigma_{m_{AB}}^2 + \left(-\frac{m_{AB}}{\Delta T_B^2}\right)^2 \cdot \sigma_{\Delta T_B}^2} \quad (3)$$

Where:

$\sigma_{CTE_{AB}}$ : The uncertainty of the coefficient of thermal expansion (mm/m/K)

$\sigma_{\Delta T_B}$ : The uncertainty of the temperature difference between the measurement series (K)

However, in the case of the 11T dipole short model coil, it was noticed that the strong bending of the coil between the measurement series M<sub>1</sub> and M<sub>2</sub> could influence the scale factor in the 7-parameter least square transformation. So, in order to get the best estimated scale factor for the expansion the following procedure has been followed:

- **1<sup>st</sup> step:** The 6 DOF (3 translations, 3 rotations, scale fixed to 1.0) transformation of series M<sub>2</sub> to get in the coordinate system of the reference measurement (M<sub>1</sub> series)
- **2<sup>nd</sup> step:** The 4 DOF transformation (2 translations in X and Z, 1 rotation around Y and 1 scale factor in XZ plane) of the transformed results of the 1<sup>st</sup> step to the warm reference measurement (M<sub>1</sub> series).
- **3<sup>rd</sup> step:** The calculated expansion of the two first steps using the XZ coordinates of all points on coil surfaces has to be corrected due to the bending of the coil. The length of the arc of the bending coil can be

calculated with the input values of the height of the arc (h) and the width of the arc (w), using the intersecting chords theorem [6], by the Eq. 6, [7]:

$$r = \frac{w^2}{8h} + \frac{h}{2} \quad (4)$$

$$C = 2 \operatorname{atan}\left(\frac{w}{2 \cdot (r-h)}\right) \quad (5)$$

$$L = C \cdot r \quad (6)$$

Where:

- r: radius of arc (m)
- C: Center angle of arc (rad)
- L: Length of the arc (m)

In the case that the arc is longer (difference of arc to straight line), the expansion has to be less than the estimated from the 2<sup>nd</sup> step by a value that is given by the next equation.

$$D = \left[\frac{L-w}{w}\right] \cdot 1000 \quad (7)$$

Where:

D: the correction of the expansion due to the bending of the coil [mm/m]

## RESULTS

The analysis of the measurement results is focused on two different parts. The first one is dedicated to the deformation analysis, which is based on a 7 - parameter least-square transformation (3 translations, 3 rotations and 1 scale factor) of the measurement series M<sub>2</sub>, M<sub>3</sub> and M<sub>4</sub> that have been transformed on the series M<sub>1</sub> (reference measurement). Also, a deformation analysis of M<sub>4</sub> series transformed on the M<sub>3</sub> series took place.

The second part of the analysis is based on the procedure to get the best-estimated scale factor of the bended coil.

### Deformation analysis

The coordinates of the measured points of the **M<sub>2</sub> (Cold), M<sub>3</sub> and M<sub>4</sub> series** have been changed using a best-fit transformation with 7 degrees of freedom (3 rotations, 3 translations and 1 scale factor) with respect to the measured points of the reference measurement **M<sub>1</sub> series** (Warm).

Table 2: The calculated scale factors

Series	Reference Series	Scale factor
M <sub>2</sub>	M <sub>1</sub>	1.002282 (± 71 μm)
M <sub>3</sub>	M <sub>1</sub>	0.999900 (± 43 μm)
M <sub>4</sub>	M <sub>1</sub>	0.999940 (± 44 μm)
M <sub>4</sub>	M <sub>3</sub>	1.000039 (± 1 μm)

At cold conditions (M2 series), with respect to the reference series (M1), the coil is curving with the ends moving upwards by  $\sim 4.85$  mm in the vertical plane YZ as illustrated in Fig. 7. In addition the coil legs (left – right, seen from the top, Fig. 6) are deforming outwards in a range of  $\pm 0.40$  mm in the horizontal plane XZ with a maximum deformation in the middle of the coil. In the loading plates zone the deformation is almost symmetric for both sides. The large deformation in Y-direction causes a smaller systematic deformation in Z-direction (see Fig. 8).

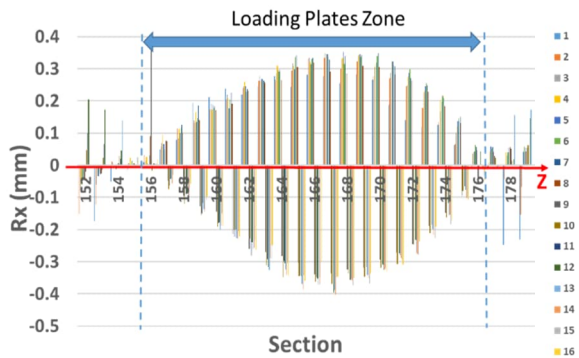


Figure 6: Residual deformation in X – direction M<sub>2</sub> To M<sub>1</sub>

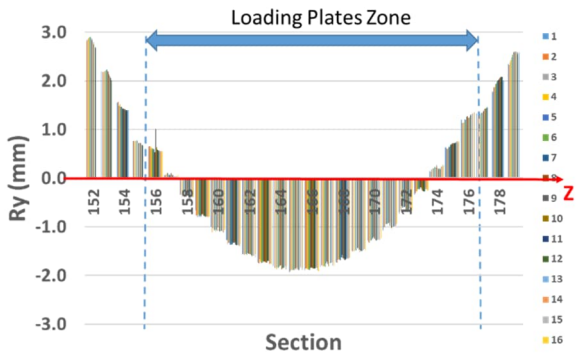


Figure 7: Residual deformation in Y – direction M<sub>2</sub> To M<sub>1</sub>

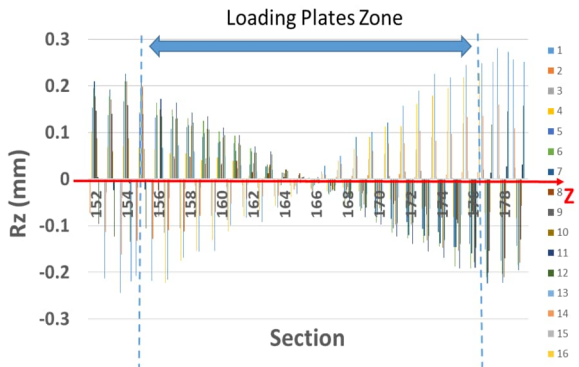


Figure 8: Residual deformation in Z – direction M<sub>2</sub> To M<sub>1</sub>

The coil shows a permanent deformation with respect to its original shape when it is back to room temperature. The coil remains curved with the ends moving upwards by  $\sim 2.94$  mm in the vertical plane YZ as illustrated in Fig. 10, and the coil legs (left-right seen from the top, Fig. 9) are

deformed outwards in a range of  $\pm 0.25$  mm in the horizontal plane XZ with a maximum deformation in the middle of the coil. Again, the large deformation in Y-direction causes a smaller systematic deformation in Z-direction (see Fig. 11).

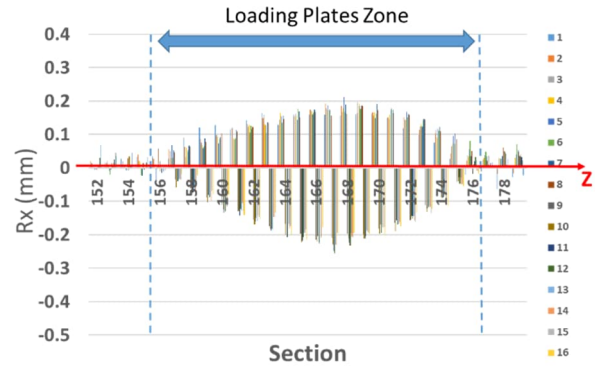


Figure 9: Residual deformation in X – direction M<sub>3</sub> To M<sub>1</sub>

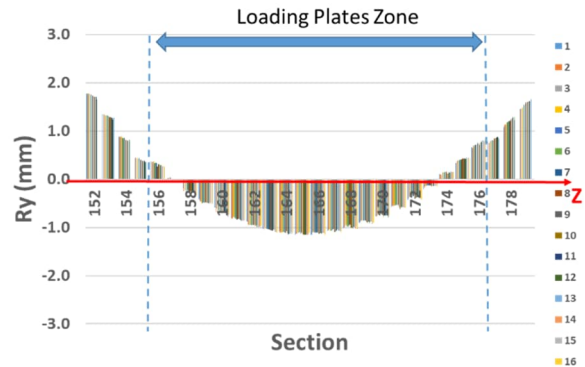


Figure 10: Residual deformation in Y – direction M<sub>3</sub> To M<sub>1</sub>

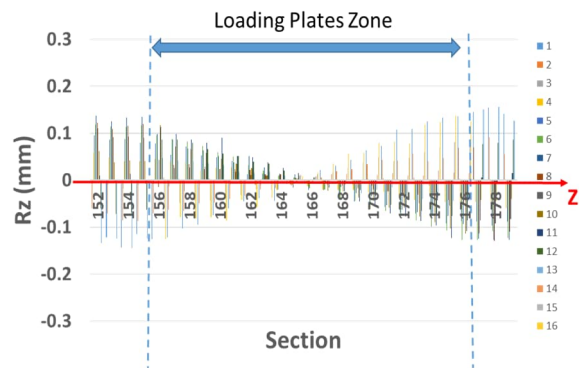


Figure 6: Residual deformation in Z–direction M<sub>3</sub> To M<sub>1</sub>

After the 7 DOF transformation of measurement series M4 to M3, it has been verified that the difference between the series M3 measurements and series M4 measurements is marginal (maximal differences less than 100  $\mu$ m) as visible in the Fig. 12-14. This fits well to the  $\Delta T$  (3.05 K) measured between these two sets of measurements, i.e. the shape of the coil can be characterized as stable compared to the bending due to the cold test.

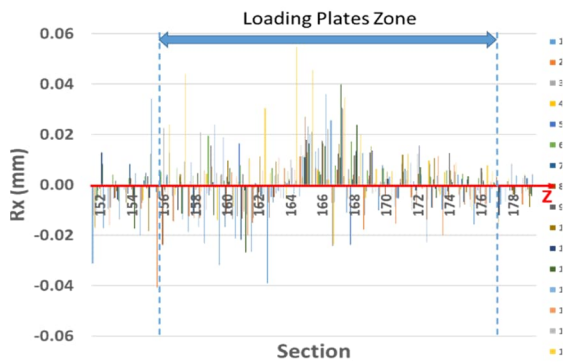


Figure 7: Residual deformation in X-direction M<sub>4</sub> To M<sub>3</sub>

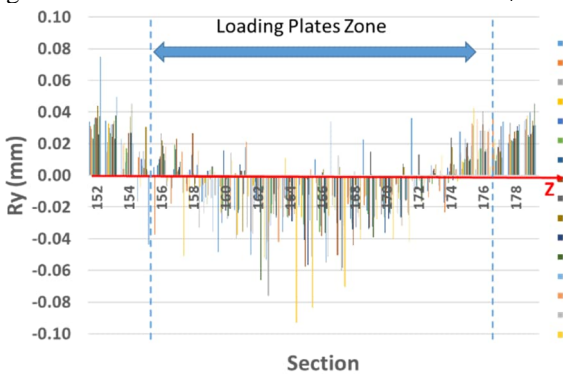


Figure 8: Residual deformation in Y-direction M<sub>4</sub> To M<sub>3</sub>

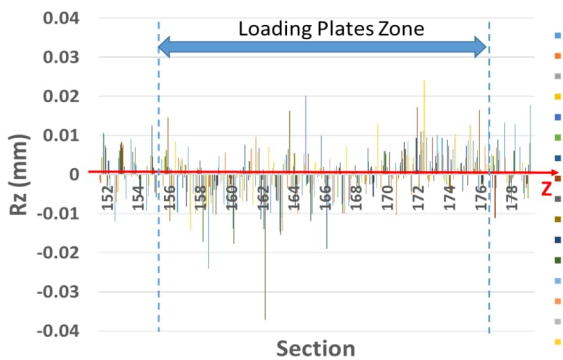


Figure 9: Residual deformation in Z-direction M<sub>4</sub> To M<sub>3</sub>

### Estimation of coefficient of thermal expansion

The best estimation of the CTE of the 11T dipole short model coil has been done accordingly to the procedure that is described in paragraph “ESTIMATION OF THE CTE” taking into account the strong bending of the coil. The scale factor (SF) of the two first steps using the XZ coordinates of all points on the different coil surfaces has been calculated  $SF_{C_{M_2 T_0 M_1}} = 12.86 \pm 0.1 \mu\text{m/m/K}$ . After applying the correction D (see Eq. 7) of the bending of the coil, the final thermal expansion coefficient is calculated  $CTE_{C_{M_2 T_0 M_1}} = 12.77 \pm 0.1 \mu\text{m/m/K}$ .

## CONCLUSION

After the four measurement series of the coil, the following conclusions can be summarized:

- The photogrammetric measurements in cryogenic condition has been successfully completed despite the

harsh environmental conditions and the 3D measurement precision has been close to the one of the room temperature measurement.

- Statistical data for image measurement precision and scale bar residuals have been at the same level for warm and cold measurements.
- The homogeneous temperature of the coil and the corresponding measurement is crucial for the setup.
- For the 11T model coil it was the first cool down cycle and the final temperature difference between warm and cold has been  $\Delta T \approx 177.68 \text{ K}$ .
- The 11T model coil is a flexible structure that contracts but also bends (4.85 mm), twists (0.26 mm) and the pole opens during the cold test ( $\pm 0.4 \text{ mm}$ ), which influences the global scale factor in the least square transformation.
- The form of the 11T dipole short model coil after the warm up is significantly different from the first warm measurement (M<sub>1</sub> series). The residual bend after the cold test is permanent and significant.
- The difference of  $39 \mu\text{m/m}$  between the two scale factors that come up from the last two warm measurements (M<sub>3</sub> and M<sub>4</sub> series) with respect to the reference warm measurement (M<sub>1</sub> series) can for a very large part be explained by the temperature difference of 3.2 K.
- The best estimate for the global CTE is  $12.8 \pm 0.3 \mu\text{m/m/K}$  for the difference from room temperature and a  $\Delta T \approx 177.68 \text{ K}$ . Due to the use of different materials for the coil construction, a single CTE is considered as a major simplification to characterize the object.

## REFERENCES

- [1] L. Rossi, O. Brüning, “Introduction to the HL-LHC Project”, Open Access chapter published by World Scientific Publishing Company and distributed under the terms of the Creative Commons Attribution Non-Commercial (CC BY-NC) 3.0 License, 2015Ch.
- [2] S. Balachandran et al, Metallographic analysis of 11 T dipole coils for the High Luminosity-Large Hadron Collider (HL-LHC), Supercond. Sci. Techno. **34** 025001, 2021
- [3] L. Bianchi, “Thermophysical and mechanical characterization of advanced materials for the LHC collimation system”, Thesis, Cern – University of Pisa, 043, 10.05.2017
- [4] B. Bordini et al., “Nb3Sn 11 T Dipole for the High Luminosity LHC (CERN)”, 2019
- [5] P. Ferracin, G. Ambrosio, et al., “The HL-LHC Low- $\beta$  quadrupole magnet MQXF: From short models to long prototypes”, IEEE Transactions on Applied Superconductivity, 29(5), p.p 1-8, 2019
- [6] J. Steiner, “Einige geometrische Betrachtungen - Primary Source Edition”, Nabu Press, 2014
- [7] Papanikolaou, “Euclidean geometry”. School Book Publishing Organization, Athens, 1978